Vol 18 No 9, September 2009
1674-1056/2009/18(09)/3934-06

Chinese Physics B

© 2009 Chin. Phys. Soc.
and IOP Publishing Ltd

Elastic stability and electronic structure of low energy tetragonal and monoclinic PdN_2 and PtN_2*

Zhao Wen-Jie(赵文杰) and Wang Yuan-Xu(王渊旭)†

Institute for Computational Materials Science and Physics Department, Henan University, Kaifeng 475004, *China*

(Received 23 December 2008; revised manuscript received 13 February 2009)

This paper studies the elastic and electronic structure properties of two new low-energy structures of PdN_2 and PtN_2 by first-principles calculations. It finds that tetragonal and monoclinic structures are more stable than a pyrite one. The always positive eigenvalues of the elastic constant matrix confirm that both the tetragonal and monoclinic structures are elastically stable. The origin of the low bulk modulus of the two structures is discussed. The results of the calculated density of states show that both of the two low-energy structures are metallic.

Keywords: palladium nitride, elastic constant, structure, electronic structure
PACC: 6220D, 7115A, 7115M

1. Introduction

Transition metal nitrides are of great interest in both fundamental science and technical applications.[1−6] From the fundamental point of view, study of their structure and stability is important because the noble metals were generally thought to be incapable of forming nitrides before the synthesis of platinum nitride under high pressures and at high temperatures. From the technological point of view, platinum nitride and other noble metal nitrides, if synthesized, may possess potentially intriguing electronic and mechanical properties. For example, platinum nitride has a bulk modulus which is comparable to that of cubic-BN, a well-known superhard material.[7]

For PtN_2, the pyrite structure was first suggested by Crowhurst to interpret the experimental Raman spectra due to its similarity to that of pyrite FeS_2. Yu *et al*[8] reported that pyrite PtN_2 is indeed elastically stable with a lower energy than fluorite PtN_2, and their calculated results match the experimental data[7] very well. Gou *et al*[9] have investigated the structural, mechanical, and electronic properties of PtN_2 with pyrite and orthorhombic FeS_2 structures. However, the low-pressure phase diagram of the PtN_2 system is still not well understood. In particular, its degree of thermodynamic stability has only been addressed briefly in Ref.[10], where it was proposed that the Pt–N compound is only metastable at low pressures. Åberg *et al*[11] address this issue by calculating the formation enthalpies of platinum nitrides as a function of pressure. They also report the discovery of two new low-energy crystal structures, which are more stable under low pressure than any of the crystal phases that have been synthesized experimentally or calculated from theory. The first structure, denoted by ST_{AA}, is simple tetragonal and belongs to space group 127 ($P4/mbm$). The second structure, ST_{AB}, is monoclinic and belongs to space group 12 (C_2/m). To our knowledge, these new crystalline phases have not been observed previously in any other compound. Although the two new crystal structures were first proposed by Åberg *et al* in Ref.[8], their elastic properties have not been investigated in detail. Here, we show that the ST_{AA} and ST_{AB} structures are indeed elastically stable with a lower energy than the pyrite structure. The electronic structure calculations reveal that both ST_{AA} and ST_{AB} PtN_2 are metallic, which is in contrast to the insulating behaviour of the pyrite structure. The elastic properties and electronic structure of PdN_2 with ST_{AA}, ST_{AB} as well as pyrite structures are also studied in the present work.

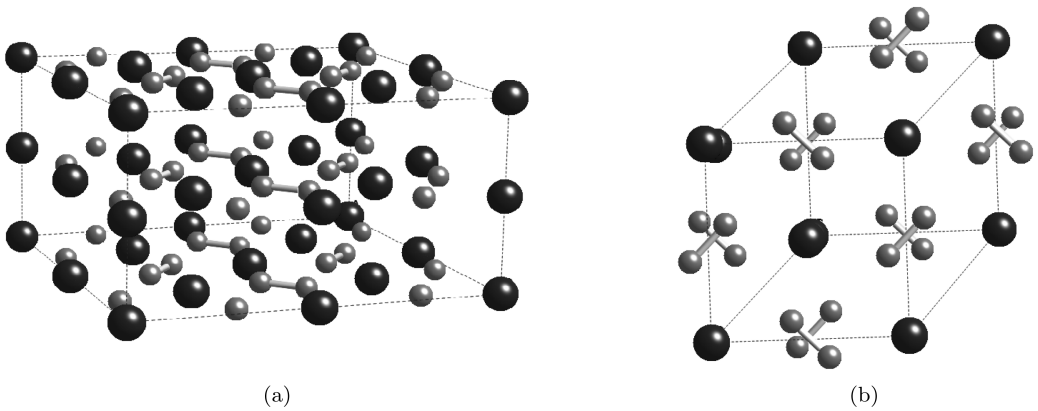
*Project supported by the Program for Science & Technology Innovation Talents in Universities of Henan Province of China (Grant No 2009HASTIT003), the Foundation of Science and Technology Department of Henan Province of China (Grant No 082300410010), and Scientific Research Foundation for the Returned Overseas Chinese Scholars, Ministry of Education of China.
†Corresponding author. E-mail: wangyx@henu.edu.cn

2. Computational details

The calculations presented in this study are performed within the density functional theory, using the projector-augmented wave (PAW) method.[12,13] We use the Vienna *ab initio* simulation program computer code,[14−16] which implements the method. The local density approximation[17] (LDA) is used with the PAW potential. The structure is optimized with the conjugate-gradient algorithm method. Increasing the plane-wave cutoff energy from 500 eV to 550 eV, we find that the change of energy is still larger than 0.005 eV. Increasing the cutoff energy from 550 eV to 600 eV, we find that the change of lattice constants is less than 0.03% and the change of energy is less than 0.005 eV. So, a plane-wave cutoff energy of 600 eV is employed throughout. The calculations are performed by using a (12,12,24) Monkhorst–Pack mesh, which corresponds to 252 k points in the irreducible part of the Brillouin zone of the ST_{AA} (symmetry No.127) structure. Furthermore, increasing the cutoff energy to 700 eV and the number of k points to (14,14,28) changes the lattice constants less than 0.03%, which indicates that these calculations are reliable. The computational conditions for the ST_{AB} (symmetry No.12) and pyrite structures are similar to the ST_{AA} one except for the different Monkhorst–Pack meshes (12,12,12). By using these computational conditions, we reach an accuracy of 5 meV/Å in the forces. The bulk modulus and its pressure derivative are obtained by fitting pressures and cell volumes with the third-order Birch Murnaghan equation of state.[18] The elastic constants are calculated by the strain-stress method. A small finite strain is applied on the optimized structure and the atomic position is optimized. Then, the elastic constants are obtained from the stress of the strained structure. The bulk modulus and the shear modulus in Table 2 are calculated by the Voigt–Reuss–Hill approximation method.[19]

3. Results and discussions

Figure 1 illustrates the two structures (first proposed in Ref.[8]) with AA and AB stacking that have lower energies than any previously proposed crystal structure for transition metal nitrides at ambient conditions. The first structure, according to Ref.[8], denoted by ST_{AA}, is simple tetragonal and belongs to space group 127 ($P4/mbm$). The metal ions occupy the $2a$ Wyckoff positions and the nitrogen atoms are located at the $4g$ positions. The second structure, ST_{AB}, is monoclinic and belongs to space group 12 (C_2/m). The metal ions occupy the $4e$ sites and the nitrogen atoms are located at the $4h$ and $4i$ positions.



(a) (b)

Fig.1. (a) Crystal structures of the ST_{AA} PdN_2. (b) The ST_{AB} PdN_2. The Pd and N atoms are represented as large and small spheres, respectively. The shortest Pd–N and N–N bonds are 2.01 Å and 1.22 Å.

Table 1 lists the calculated equilibrium lattice parameters, cell volume, the relative total energy, the bulk modulus, and its pressure derivative of PdN_2 and PtN_2 with the three structures. The calculated lattice parameters a, 4.785 Å, for pyrite PtN_2 with LDA are in excellent agreement with the experimen-

tal data, 4.800 Å [10] and 4.804 Å,[7] with an error of about 0.31% and 0.39%, respectively. Also, the lattice parameters of pyrite PtN_2 are consistent with the different theoretical results.[8,9] This indicates that the computations are reliable to represent the crystal structure. The bulk modulus B was obtained by allowing the pressure derivative B′ to freely vary. Because B′ is higher than those obtained for most materials, we can only conclude that the actual bulk modulus is larger than the value of B. For example, the actual bulk modulus of ST_{AA} PdN_2 should be larger than 107 GPa. From this table, it can be seen that the ST_{AA} structure is more stable in energy than the ST_{AB} and pyrite ones. However, it is a pity that the ST_{AA} phase has a much larger cell volume than the pyrite one; this fact results in the lower bulk modulus of the ST_{AA} structure. The calculated results (shown in Table 1) show that, for PtN_2, the ST_{AA} structure also has a lower energy and much larger cell volume than the pyrite one. Although the ST_{AA} structure has a slightly smaller cell volume than the ST_{AB} one, the cell volumes for both of them are much larger than the pyrite one. Thus, the bulk moduli for both the ST_{AA} and ST_{AB} structures are evidently smaller than those of the pyrite one. The bulk modulus of pyrite PtN_2, 354 GPa, is very close to the experimental value of 354–372 GPa[7] and the theoretical value of 352 GPa.[8] To understand the high stability of the ST_{AA} and ST_{AB} phases in comparison with the pyrite one, we discuss the inter-atomic distances. For both the ST_{AA} and ST_{AB} PdN_2, the nearest Pd–N (2.01 Å) and N–N (1.22 Å) distances are smaller than the corresponding values of 2.12 Å and 1.28 Å for pyrite PdN_2. A similar situation is found for PtN_2, the nearest Pt–N and N–N bonds for both of the ST_{AA} and ST_{AB} phases are 2.00 Å and 1.25 Å, respectively, which are also smaller than the corresponding values of 2.07 Å and 1.40 Å for the pyrite phase. Thus, for both PdN_2 and PtN_2, the ST_{AA} and ST_{AB} phases are lower in energy than the pyrite ones.

Table 1. Calculated equilibrium lattice parameters, a (in Å), c (in Å), cell volume V (in Å^3), relative energy E (in eV), bulk modulus B (in GPa), and its pressure derivative at zero pressure (B') of PdN_2 and PtN_2. V and E are per chemical f.u.

		a	c	V	E	B	B'
PdN_2	ST_{AA}	4.796	2.869	66.00	0	107	6.30
	ST_{AB}	6.781	10.579	66.49	0.05	106	6.56
	pyrite	4.843		56.66	0.68	156	9.48
PtN_2	ST_{AA}	4.777	2.828	64.53	0	157	7.45
	ST_{AB}	6.748	10.509	65.45	0.06	124	8.96
	pyrite	4.785		54.77	0.65	354	5.01
	pyrite (Expt, Ref.[7])	4.804		55.43		354	5.26
	pyrite (Theory, Ref.[8])	4.770		54.27		352	5.20
	pyrite (Theory, Ref.[9])	4.820		55.99			
	pyrite (Expt, Ref.[10])	4.800		54.95		350–410	

From Table 2, except pyrite PtN_2, the bulk modulus does not agree well with those from the third-order Birch–Murnaghan equation of state.[18] We note that the pressure derivative (shown in Table 1) deviates to a great extent from the canonical value of 4, thus we use the results (shown in Table 2) from the Voigt–Reuss–Hill approximation method.[19] We also calculated the eigenvalues of the elastic constant matrix of the two materials and found that all eigenvalues are positive, which indicates that the ST_{AA}, ST_{AB}, and pyrite structures of the two materials are all elastically stable. The small elastic constant c_{33} (124 GPa) of ST_{AA} PdN_2 implies that it can be easily compressed along the z-axis; this fact results from the layer structure. The small c_{44} (13 GPa) shows the weak resistance ability for PdN_2 against an applied (001) shear deformation. From our calculations, the volumes of both pyrite PdN_2 and PtN_2 structures are smaller than those of the ST_{AA} and ST_{AB} phases. The bulk modulus 187 GPa of pyrite PdN_2 is slightly larger than that of the ST_{AA} (135 GPa) and ST_{AB} (134 GPa) ones, while the bulk modulus 351 GPa of pyrite PtN_2

is about 2 times of that of the ST_{AA} (188 GPa) and ST_{AB} (183 GPa) ones. More interestingly, the bulk modulus 351 GPa of pyrite PtN_2 is about two times of that of pyrite PdN_2 (187 GPa). Such a contrast between the bulk moduli of pyrite PdN_2 and PtN_2 implies that there may be other ST_{AA} or ST_{AB} transition metal dinitrides with higher moduli as compared to the ST_{AA} and ST_{AB} PdN_2 structures.

Table 2. Calculated elastic constants (in GPa). Bulk modulus B (in GPa), shear modulus G (in GPa), and G/B of PdN_2 and PtN_2.

		c_{11}	c_{12}	c_{13}	c_{22}	c_{23}	c_{33}	c_{44}	c_{55}	c_{66}	B	G	G/B
PdN_2	ST_{AA}	593	115	9			124	13		106	135	67	0.49
	ST_{AB}	333	91	126	391	122	142	91	122	127	134	67	0.50
	pyrite	333	24					70			187	107	0.84
PtN_2	ST_{AA}	892	164	27			134	22		154	188	100	0.53
	ST_{AB}	501	140	186	591	182	201	131	176	181	183	100	0.55
	pyrite	820	116					144			351	230	0.66
	pyrite (Theory, Ref.[8])	824	117					152			352	214	0.61
	pyrite (Theory, Ref.[9])	842	120					152			361	236	0.65

The electronic structures of PdN_2 and PtN_2 at zero pressure are calculated. Figure 2 shows the total and partial density of states (DOS). No energy gap is seen for the ST_{AA} and ST_{AB} structures, indicating a metallic nature of ST_{AA} and ST_{AB} palladium nitride. There are deep minima in DOS at the Fermi level, giving a DOS at the Fermi level $[N(E_F)]$ of only 0.65 and 0.5 states/eV unit cell for the ST_{AA} and ST_{AB} structures, respectively. The low $N(E_F)$ indicates that ST_{AA} and ST_{AB} palladium nitride are poor metals, in contrast with the semiconducting property of the pyrite phase. The DOS distribution shown in Fig.2 manifests a typical stability effect by the formation of a pseudogap, where the decrease of the total DOS at the Fermi level is accompanied by the shifting of occupied bonding states to lower energies and unoccupied antibonding states to higher energies. For the ST_{AA} phase, the states from −13 eV to −11 eV

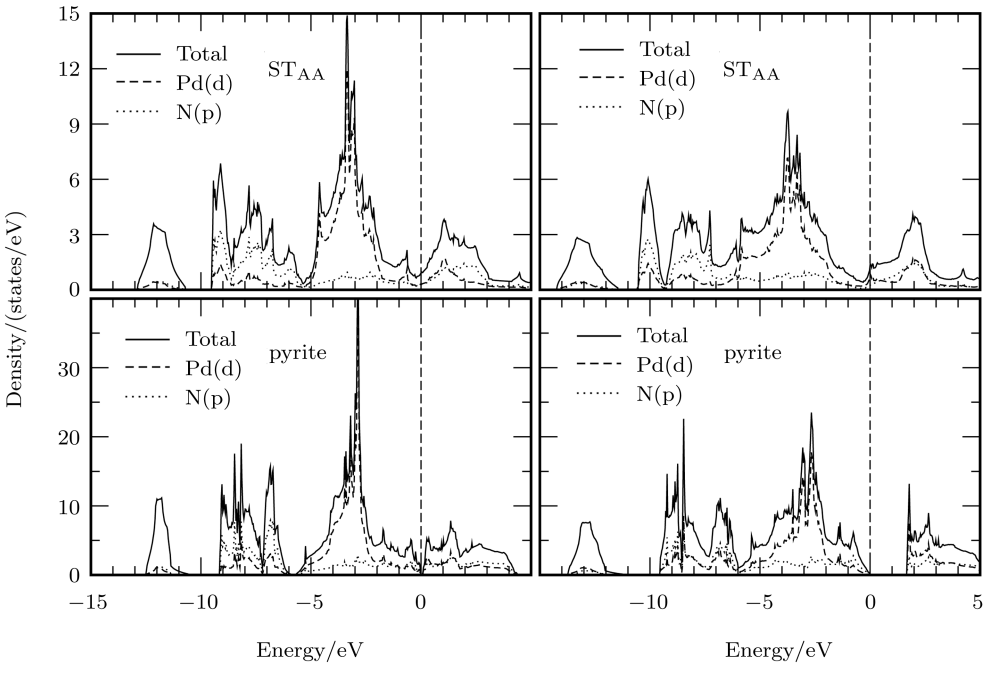


Fig.2. Total and partial DOS of PdN_2 and PtN_2. The Fermi level corresponds to the vertical dashed line.

are mainly composed of N(2s) states. The states above −9 eV are mainly composed of Pd(4d) states and N(2p) states. Due to the stronger Pd(t_{2g})–N(2p) interactions, the t_{2g} band has a larger dispersion than that of the e_g band, with the antibonding part almost empty. Also, the charge density distributions of ST_{AA} PdN_2 have been given to make sense of the bonding properties. From Fig.3, we find that strong covalency is present in the interstitial dinitrogen units for the ST_{AA} phase, and weaker directional bonding between Pd–N exists in PdN_2, which may explain the high stability and low bulk modulus of the ST_{AA} phase.

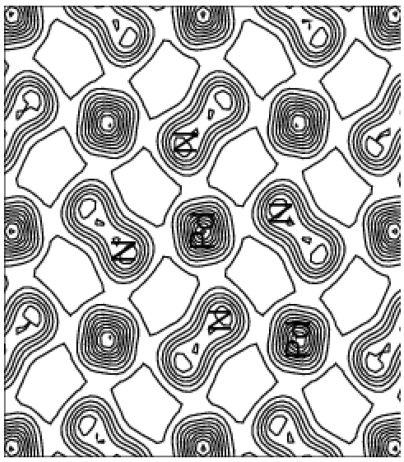


Fig.3. The charge density corresponding to the valence bands from −10 to 0 eV for the ST_{AA} PdN_2. It is drawn on the (001) plane.

Figure 4 shows the calculated relative enthalpy between the ST_{AA} phase and the pyrite one. As seen in Fig.4, the enthalpy change is mainly determined by $P\Delta V$. The bulk modulus of the pyrite structure, which is higher in energy under ambient conditions, is larger than that of the ST_{AA} phase. Thus, with the increase of pressure, the change of $P\Delta V$ for the ST_{AA} phase is relatively significant in comparison to that of the pyrite ones. The ST_{AA} structure for PdN_2 and PtN_2 are stable up to 13 GPa, which is in good agreement with that reported in Ref.[11].

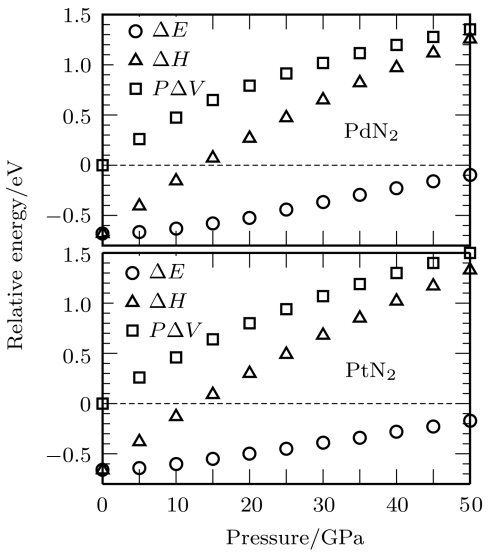


Fig.4. Enthalpy changes ΔH of PdN_2 and PtN_2 in the ST_{AA} and pyrite phases as a function of pressure. The enthalpy of the pyrite structure is taken as a reference level.

4. Conclusions

The stabilities of PdN_2 and PtN_2 have been investigated by using first-principles calculations. We find that they can be stabilized in the ST_{AA} and ST_{AB} structures, in which the metal ions occupy simple tetragonal lattice sites. The calculated results of the pyrite PtN_2 are in agreement with the available values, and ST_{AA} PdN_2 and PtN_2 are more energetically stable under ambients condition than the pyrite structure. The results of the calculated DOS indicate that both PdN_2 and PtN_2 are metallic in the ST_{AA} and ST_{AB} phases. Moreover, the bulk modulus and shear modulus for ST_{AA} and ST_{AB} PtN_2 are much smaller than those of the pyrite structure. It is interesting to know if other transition metal nitrides and carbides can be stabilized in the ST_{AA} and ST_{AB} structures. The calculations are in progress and the results will be published elsewhere.

References

[1] Chun J S, Petrov I and Greene J E 1999 *J. Appl. Phys.* **86** 3633

[2] Al-Brithen H and Smith A R 2000 *Appl. Phys. Lett.* **77** 248

[3] Kroll P 2003 *Phys. Rev. Lett.* **90** 125501

[4] Ranjan V, Bellaiche L and Walter E J 2003 *Phys. Rev. Lett.* **90** 257602

[5] Wang S Y, Duan G Y, Qiu J H, Jia Y and Chen L Y 2006 *Acta. Phys. Sin* **55** 1979 (in Chinese)

[6] Liang Y C, Guo W L and Fang Z 2007 *Acta. Phys. Sin.* **56** 4847 (in Chinese)

[7] Gregoryanz E, Sanloup C, Somayazulu M, Badro J, Fiquet G, Mao H K and Hemley R J 2004 *Nat. Mater.* **3**

294

[8] Yu R, Zhan Q and Zhang X F 2006 *Appl. Phys. Lett.* **88** 051913

[9] Gou H Y, Hou L, Zhang J W, Sun G F, Gao L H and Gao F M 2006 *Appl. Phys. Lett.* **89** 141910

[10] Crowhurst J C, Goncharov A F, Sadigh B, Evans C L, Morrall P G, Ferreira J L and Nelson A J 2006 *Science* **311** 1275

[11] Åberg D, Sadigh B, Crowhurst J and Goncharov A F 2008 *Phys. Rev. Lett.* **100** 095501

[12] Kresse G and Joubert D 1999 *Phys. Rev.* B **59** 1758

[13] Blöchl P E 1994 *Phys. Rev.* B **50** 17953

[14] Kresse G and Hafner J 1993 *Phys. Rev.* B **47** R558

[15] Kresse G and Hafner J 1994 *J. Phys.*: *Condens. Matter* **6** 8245

[16] Kresse G and Furthmller J 1996 *Phys. Rev.* B **54** 11169

[17] Ceperley D M and Alder B J 1980 *Phys. Rev. Lett.* **45** 566

[18] Birch F 1947 *Phys. Rev.* **71** 809

[19] Hill R 1952 *Proc. Phys. Soc. London* **65** 349